J. Phys. D: Appl. Phys. **42** (2009) 075308 (5pp) doi:10.1088/0022-3727/42/7/075308

High-barrier rectifying contacts on undoped ZnO films with $(NH_4)_2S_x$ treatment owing to Fermi-level pinning

Yow-Jon Lin[1,3], Shih-Sheng Chang[1], Hsing-Cheng Chang[2] and Yang-Chun Liu[1]

[1] Institute of Photonics, National Changhua University of Education, Changhua 500, Taiwan
[2] Department of Automatic Control Engineering, Feng Chia University, Taichung 407, Taiwan

E-mail: rzr2390@yahoo.com.tw (Y J Lin)

Received 2 November 2008, in final form 7 February 2009
Published 20 March 2009
Online at stacks.iop.org/JPhysD/42/075308

Abstract

We report on the formation of high-barrier Ti and Ni contacts to $(NH_4)_2S_x$-treated ZnO films grown by pulsed-laser deposition. The x-ray photoelectron spectroscopy (XPS) results show that the position of the Zn 3d core-level peak at the $(NH_4)_2S_x$-treated ZnO surface is the same as that at the Ti/$(NH_4)_2S_x$-treated ZnO or Ni/$(NH_4)_2S_x$-treated ZnO interfaces, suggesting the occurrence of Fermi-level (E_F) pinning and the formation of a barrier height of ~2.7 eV. From the photoluminescence and XPS measurements, it is suggested that a high Zn-vacancy density might cause the ZnO E_F to be pinned close to the Zn-vacancy defect level at approximately 0.7 eV above the valence band maximum. In addition, the discrepancy in barrier-height values obtained from XPS and current–voltage measurements suggests the formation of S–Zn surface dipoles with S atoms on the surfaces.

(Some figures in this article are in colour only in the electronic version)

1. Introduction

ZnO has a 3.4 eV direct gap at room temperature [1] and has attracted much interest for its application in optoelectronic devices [2–10]. Other devices that have been demonstrated so far include ultraviolet Schottky barrier photodetectors, Schottky diodes and metal–semiconductor field effect transistors [11–23]. High-barrier rectifying contacts are required for improving these devices. Recent review and studies of rectifying contact properties on ZnO have appeared [12–19, 24, 25]. Some reported values for barrier height (ϕ_B) for different metals are 0.7–0.8 eV for Pt [13, 15], 0.6–0.7 eV for Au [12, 16], 0.56–0.69 eV for Ag [14, 16], 1.20 eV for AgO_x [18], 0.65 eV for Ir [19] and 0.60–1.16 eV for Pd [14, 17, 19]. There is a fairly large discrepancy in reported values. The magnitude of the metal's influence on Schottky barriers electrically correlates directly with the metal reactivity and the defect densities at the surface and ZnO bulk. A rectifying junction fabricated on ZnO surfaces with a conducting polymer as a high work function metal electrode have been reported by Gunji *et al* [20] and Mridha and Basak [21]. In this paper, we report on the formation of high-barrier rectifying contacts on $(NH_4)_2S_x$-treated undoped ZnO films grown by pulsed-laser deposition (PLD). According to the experimental results, we found the same ϕ_B of the Ti/$(NH_4)_2S_x$-treated ZnO samples as that of the Ni/$(NH_4)_2S_x$-treated ZnO samples, suggesting Fermi-level (E_F) pinning at the metal/ZnO interfaces. We suggested that a high Zn-vacancy (V_{Zn}) density induced by $(NH_4)_2S_x$ treatment might cause the ZnO E_F to be pinned close to the V_{Zn} defect level at approximately 0.7 eV above the valence band maximum (VBM).

2. Experiment procedure

A 600 nm ZnO film grown on a (0 0 0 1) sapphire substrate by PLD is used in this study. In previous studies [26–30], undoped and doped ZnO films were fabricated by PLD. A KrF excimer laser (wavelength of 248 nm) was employed and the beam was focused to produce an energy density of 5–7 J cm^{-2} at 10 Hz repetition rate on a commercial hot pressed stoichiometric ZnO (99.999% purity) target. The films were deposited at a growth rate of 94.25 nm h^{-1} at 550 °C substrate temperature and a base vacuum of 1.2×10^{-8} Torr. No oxygen gas flow was introduced

[3] Author to whom any correspondence should be addressed.

during the process of growth. According to the Van der Pauw–Hall measurements, we found that the electron concentration and the mobility were calculated to be $4.3 \times 10^{17}\,\mathrm{cm}^{-3}$ and $12\,\mathrm{cm}^2\,\mathrm{V}^{-1}\,\mathrm{s}^{-1}$, respectively. These grown ZnO samples were cleaned with chemical solutions of trichloroethylene, acetone and methanol. Then the samples were rinsed with deionized water and immediately blown dry with N_2. After drying under a dry nitrogen flow, some of the ZnO samples were next dipped into a yellow 60 °C $(NH_4)_2S_x$ solution (purchased from Nippon Shiyaku) for 3 min (referred to as $(NH_4)_2S_x$-treated ZnO). Next, the Ti and Ni films were, respectively, deposited on the $(NH_4)_2S_x$-treated ZnO surfaces using an electron beam evaporator. The deposited Ti or Ni layer was very thin (2 nm); therefore, the interfacial x-ray photoelectron spectroscopy (XPS) data could be directly obtained without a sputter etching treatment. XPS was employed to examine the changes in the surface band bending of ZnO, chemical bonding states of ZnO and the band bending in ZnO near the Ti/ZnO (or Ni/ZnO) interface. The VBM position (E_v) of ZnO samples with or without $(NH_4)_2S_x$ treatment and the position (E_{Zn3d}) of the Zn 3d core-level peak at the $(NH_4)_2S_x$-treated ZnO surfaces before or after metal deposition were determined from XPS measurements. The surface band bending was determined by the location of the energy of the VBM in photoemission from the sample. The XPS system was equipped with a monochromatic Al Kα source. We took a Au $4f_{7/2}$ peak or a C 1s peak for energy reference purposes. All binding energies are measured relative to E_F. Using a Ne–Cu laser (the 248.6 nm line) as an excitation source, the photoluminescence (PL) band was observed for ZnO samples at room temperature (Wide Bandgap MiniPL Spectrometer, Photon Systems). To note the change in the current–voltage (I–V) characteristic, planar-type Schottky diodes were fabricated. Using the lift-off technique, Ti (80 nm) ohmic contacts and Ti (80 nm) (or Ni (50 nm)) rectifying contacts were deposited on the ZnO surfaces with or without $(NH_4)_2S_x$ treatment, respectively. The measured device structures consisted of circular rectifying dots (diameter = 200 μm) separated radially by 100 μm from the ohmic contacts. The diodes were measured by the I–V method using a Keithley Model-4200 semiconductor characterization system.

3. Experimental results and discussion

Figure 1 shows the valence-band spectra at the ZnO surface with and without $(NH_4)_2S_x$ treatment. E_v is determined by extrapolating two solid lines from the background and the straight cutoff in the spectra [31, 32]. For ZnO samples without $(NH_4)_2S_x$ treatment, E_v was measured to be 3.52 eV. For ZnO samples with $(NH_4)_2S_x$ treatment, E_v was measured to be 0.71 eV. Comparing the ZnO samples without $(NH_4)_2S_x$ treatment, we found that E_F shifted towards VBM by 2.81 eV for ZnO samples with $(NH_4)_2S_x$ treatment. The E_F shift corresponds to an increase in the upward band bending. It is worth noting that $(NH_4)_2S_x$ treatment may lead to a marked increase in the upward band bending, owing to the creation of V_{Zn}-related defects at the ZnO surface [13].

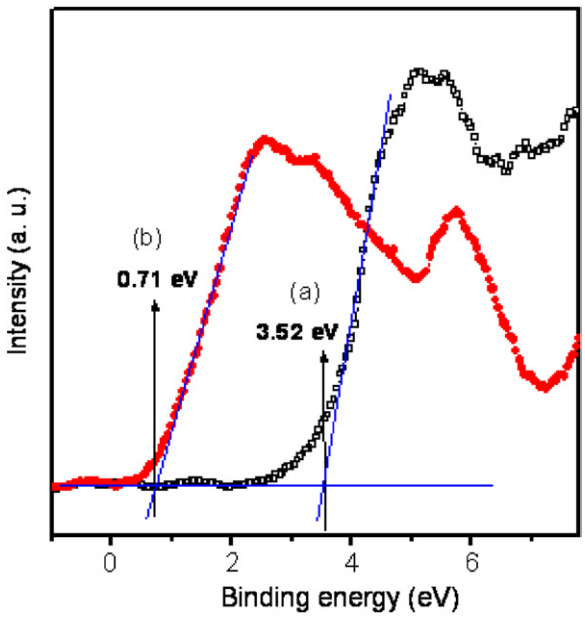

Figure 1. Valence-band spectra at the ZnO surfaces (a) without and (b) with $(NH_4)_2S_x$ treatment.

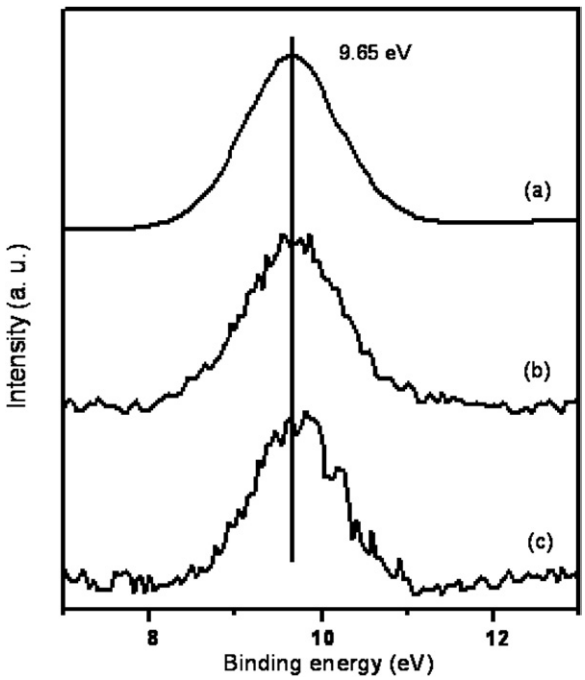

Figure 2. (a) Zn 3d core-level spectra at the $(NH_4)_2S_x$-treated ZnO surface and Zn 3d core-level spectra obtained from the (b) Ni/$(NH_4)_2S_x$-treated ZnO and (c) Ti/$(NH_4)_2S_x$-treated ZnO interface regions.

Figure 2 shows the Zn 3d core-level XPS spectra at the $(NH_4)_2S_x$-treated ZnO surface. Figure 2 also shows the Zn 3d core-level XPS spectra at the Ti/$(NH_4)_2S_x$-treated ZnO and Ni/$(NH_4)_2S_x$-treated ZnO interfaces. For ZnO samples with $(NH_4)_2S_x$ treatment, E_{Zn3d} was observed at 9.65 eV. In addition, in figure 2, we can see that E_{Zn3d} at the Ti/ZnO (Ni/ZnO) interface is located at 9.65 (9.65) eV, suggesting the presence of E_F pinning at the interfaces. In practice, most semiconductors have a much weaker dependence of ϕ_B on the

metal work function. This is often attributed to E_F pinning by interface states. According to the XPS results shown in figures 1 and 2, we deduce that a high V_{Zn} density causes the ZnO E_F to be pinned close to the V_{Zn} defect level at 0.71 eV above the VBM.

Figure 3 shows PL spectra of the ZnO film with and without $(NH_4)_2S_x$ treatment. One emission peak at room temperature was observed for ZnO samples without $(NH_4)_2S_x$ treatment and two emission peaks at room temperature were observed for ZnO samples with $(NH_4)_2S_x$ treatment. This result provides direct evidence of the deposition of a good-quality ZnO film. The peak at 3.42 eV is near band edge emission, the so-called ultraviolet luminescence. For ZnO samples with $(NH_4)_2S_x$ treatment, we find the blue luminescence (peak position at 2.72 eV) related to the V_{Zn}-related emission. The peaks are determined by Lorentzian fitting. Zn vacancies are believed to be the dominant deep acceptor states in ZnO [33, 34]. First-principles calculations also predict that V_{Zn} is the dominant native defect in *n*-type and especially oxygen-rich ZnO with the -/2- energy level at 0.8 eV above the VBM [35]. Patterson [36] pointed out that the V_{Zn} transition level is approximately 0.8 eV above the VBM. Bylander [37] stated that the V_{Zn} defect level was at approximately 0.7 eV above the VBM. Thus, we infer that the 2.72 eV luminescence transition is from the conduction band edge to the acceptor-like V_{Zn}-related level at approximately 0.7 eV above the VBM which is in agreement with the XPS result (shown in figure 1) and the reported results by Kohan *et al* [35], Patterson [36] and Bylander [37]. On the other hand, according to the results shown in figures 1 and 3, we find that the light downward band bending is formed at the ZnO surface without $(NH_4)_2S_x$ treatment and the strong upward band bending is formed at the ZnO surface with $(NH_4)_2S_x$ treatment (assuming a band gap of 3.42 eV). Therefore, ϕ_B of the Ti/ZnO (Ni/ZnO) sample was calculated to be 2.71 (2.71) eV, which is higher than the Schottky limit. This implies that E_F pinning induced by $(NH_4)_2S_x$ treatment leads to enhancing $q\phi_B$. In this study, ϕ_B of 2.71 eV was achieved on the $(NH_4)_2S_x$-treated ZnO film which is the highest reported for undoped ZnO samples.

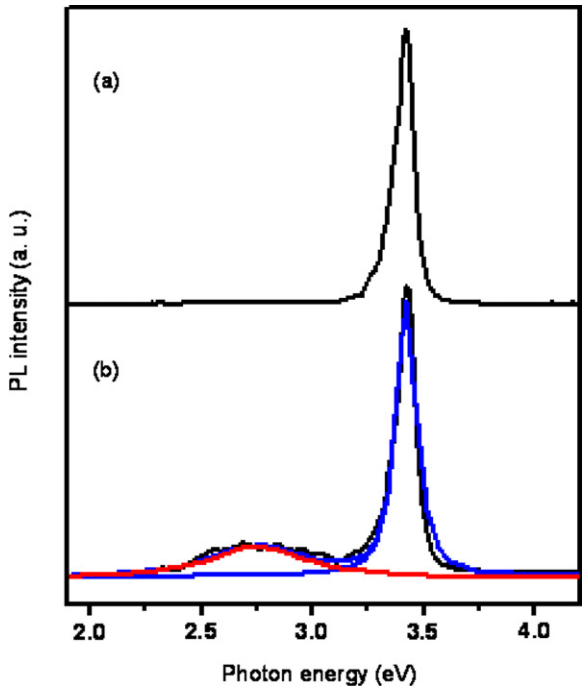

Figure 3. PL spectra of ZnO samples (*a*) without and (*b*) with $(NH_4)_2S_x$ treatment.

Figure 4(*a*) shows the current density–voltage (J–V) characteristics of the Ni/ZnO and Ti/ZnO diodes without $(NH_4)_2S_x$ treatment. The linear J–V curve indicates the formation of ohmic contacts. Figure 4(*b*) shows the rectifying J–V characteristics under forward bias condition for the Ti/$(NH_4)_2S_x$-treated ZnO and Ni/$(NH_4)_2S_x$-treated ZnO diodes. The fitting curve of the J–V characteristics in the thermionic emission (TE) or thermionic field emission (TFE) regime is also shown in Figure 4(*b*). From TE theory, the J–V characteristic of a Schottky diode is given by [38]

$$J = A^*T^2 \exp\left(-\frac{\phi_B}{kT}\right) \exp\left(\frac{qV}{nkT}\right) \qquad (1)$$

where T is the measurement temperature, k is the Boltzmann constant, q is the electron charge and A^* is the effective Richardson constant (32 A cm^{-2} K^{-2} for n-type ZnO [14]). The ideality factors (n) and ϕ_B were obtained from the

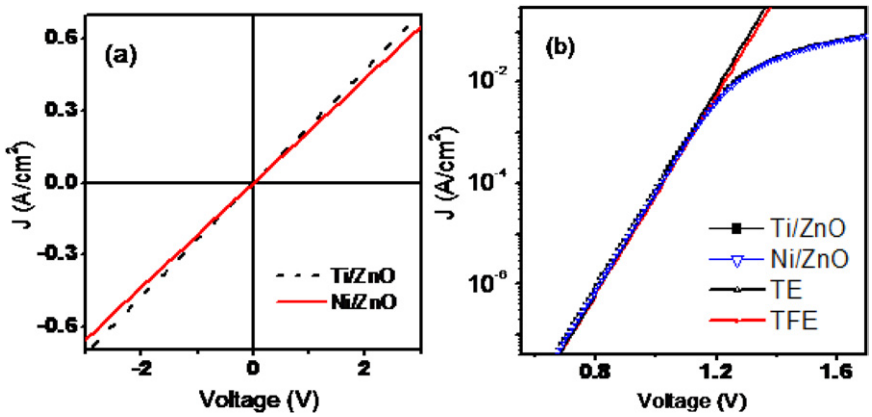

Figure 4. (*a*) J–V curves of the Ni/ZnO and Ti/ZnO diodes without $(NH_4)_2S_x$ treatment. (*b*) J–V curves of the Ni/$(NH_4)_2S_x$-treated ZnO and Ti/$(NH_4)_2S_x$-treated ZnO diodes under forward bias condition and the fitting curves to the J–V characteristic in the TE and TFE regimes.

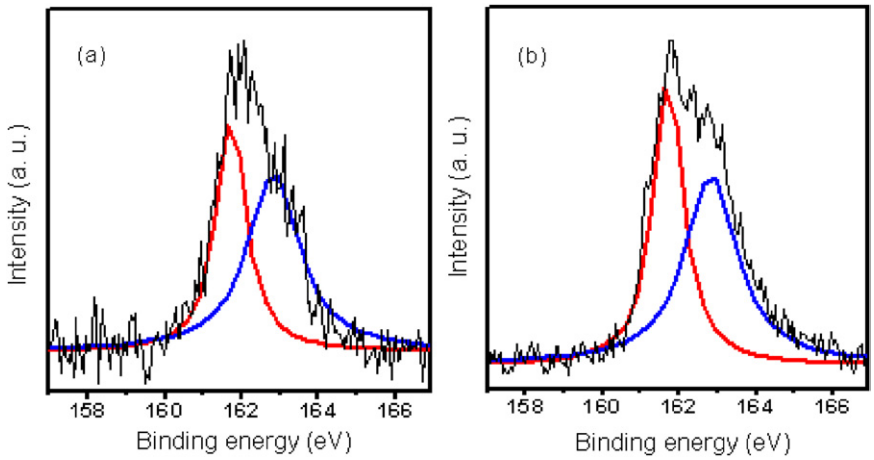

Figure 5. S 2p core-level spectra obtained from the (*a*) Ti/$(NH_4)_2S_x$-treated ZnO and (*b*) Ni/$(NH_4)_2S_x$-treated ZnO interface regions.

forward J–V characteristics, according to equation (1). ϕ_B is 1.23 eV; while n is 1.66 for the Ti/$(NH_4)_2S_x$-treated ZnO or Ni/$(NH_4)_2S_x$-treated ZnO diodes. The finding could be explained in terms of an increase in the tunnelling transport [39, 40]. Therefore, the tunnelling current was induced, making TE theory inapplicable in this case. The TFE model involving the forward current transport with a tunnel component is proposed to account for the larger n. From TFE theory, the J–V characteristic of a Schottky diode is given by [31, 38, 41]

$$J = \frac{A^*T[\pi E_{OO}(\phi_B - qV - \xi)]^{0.5}}{k\cosh(E_{OO}/kT)} \times \exp\left[-\frac{\xi}{kT} - \frac{(\phi_B - \xi)}{E_O}\right]\exp\left(\frac{qV}{E_O}\right), \quad (2)$$

$$E_O = E_{OO}\coth\left(\frac{E_{OO}}{kT}\right) = nkT. \quad (3)$$

E_{OO} is the tunnelling parameter. ξ is the energy difference between the conduction band minimum and E_F in the bulk. ϕ_B is 2.10 eV, while n (E_{OO}/kT) is 1.66 (1.50) for the Ti/$(NH_4)_2S_x$-treated ZnO or Ni/$(NH_4)_2S_x$-treated ZnO diodes based on the TFE mechanism. It is worth noting that the TFE becomes important when $E_{OO}/kT \approx 1$ and the TE important if $E_{OO}/kT \ll 1$. We find that tunnelling can be described by means of equations (2) and (3) and E_{OO} may be related to the probability of defect-assisted tunnelling [42]. This can probably be attributed to the presence of deep level defects related to E_F pinning. The discrepancy in barrier-height values obtained from XPS and J–V measurements suggests the existence of an interfacial dipole layer. The interfacial dipole (Δ) was previously taken into account by Ishii *et al* [43] and Agrawal and Ghosh [44] for the calculation of the barrier heights of electron injection. Therefore, the J–V characteristic in the presence of Δ and tunnelling can be described by the relation

$$J = \frac{A^*T[\pi E_{OO}(\phi_B + \Delta - qV - \xi)]^{0.5}}{k\cosh(E_{OO}/kT)} \times \exp\left[-\frac{\xi}{kT} - \frac{(\phi_B + \Delta - \xi)}{E_O}\right]\exp\left(\frac{qV}{E_O}\right). \quad (4)$$

Δ was calculated to be approximately −0.6 eV. In combination with the electric field induced between the metal and ZnO, the dipole has the effect of lowering the barrier height. This effect leads to an increased current. Interface dipoles may be the result of a net charge transfer across the interface due to chemical bonding [45]. It is known that the passivation of GaAs (1 0 0) surfaces by S atoms terminates the chemically active sites, leading to the formation of S–Ga surface dipoles with S atoms on the surfaces [45]. Figure 5 shows the S 2p core-level spectra obtained from the Ti/$(NH_4)_2S_x$-treated ZnO and Ni/$(NH_4)_2S_x$-treated ZnO interface region. The $2p_{3/2}$ and $2p_{1/2}$ peaks are determined by Lorentzian fitting. The $2p_{3/2}$ component is located at ∼162.0 eV. This implies the formation of S–ZnO bonds at the $(NH_4)_2S_x$-treated ZnO surfaces [13], resulting in the formation of S–Zn surface dipoles with S atoms on the surfaces.

4. Conclusions

In summary, we have analysed the ϕ_B of rectifying contacts to $(NH_4)_2S_x$-treated undoped ZnO samples using XPS and J–V measurements. High-barrier Schottky contact formation in the Ti or Ni contact to the $(NH_4)_2S_x$-treated undoped ZnO film grown by PLD was achieved in this study. The XPS results show the same ϕ_B ($\phi_B = 2.71$ eV) of the Ti/$(NH_4)_2S_x$-treated ZnO samples as of the Ni/$(NH_4)_2S_x$-treated ZnO samples, suggesting the presence of E_F pinning at the interfaces. The XPS results also show that a high V_{Zn} density causes the ZnO E_F to be pinned close to the V_{Zn} defect level at 0.71 eV above the VBM, leading to the formation of the strong upward band bending and high barrier at the metal/$(NH_4)_2S_x$-treated ZnO interfaces. The PL results show the presence of the 2.72 eV emission for the $(NH_4)_2S_x$-treated undoped ZnO samples, implying that the 2.72 eV luminescence transition is from the conduction band edge to the V_{Zn}-related level at approximately 0.7 eV above the VBM. This provides the evidence that a number of V_{Zn}-related defects existed at the $(NH_4)_2S_x$-treated ZnO surfaces, resulting in the formation of E_F pinning. In addition, the discrepancy in barrier-height values obtained from XPS and J–V measurements suggests the formation of S–Zn surface dipoles with S atoms on the surfaces. This

concept can be extended to understand and control Schottky barrier formation in other compound semiconductors as well and will be presented in future publications.

Acknowledgments

The authors acknowledge the support of the National Science Council of Taiwan (Contract No 97-2628-M-018-001-MY3) in the form of grants and thank W F Hsieh, C–H Hsu and W–R Liu (Department of Photonics and Institute of Electro-optical Engineering, National Chiao Tung University) for providing the ZnO samples.

References

[1] Yang H S, Norton D P, Pearton S J and Ren F 2005 *Appl. Phys. Lett.* **87** 212106
[2] Tan S T, Sun X W, Zhao J L, Iwan S, Cen Z H, Chen T P, Ye J D, Lo G Q, Kwong D L and Teo K L 2008 *Appl. Phys. Lett.* **93** 013506
[3] Chang C Y, Tsao F C, Pan C J, Chi G C, Wang H T, Chen J J, Ren F, Norton D P and Pearton S J 2006 *Appl. Phys. Lett.* **88** 173503
[4] Jeong M C, Oh B Y, Ham M H and Myoung J M 2006 *Appl. Phys. Lett.* **88** 202105
[5] Park S H K, Lee J I, Hwang C S and Chu H Y 2005 *Japan. J. Appl. Phys.* **44** L242
[6] Alivov Y I, Nostrand J E V, Look D C, Chukichev M V and Ataev B M 2003 *Appl. Phys. Lett.* **83** 2943
[7] Yuen C, Yu S F, Lau S P, Rusli and Chen T P 2005 *Appl. Phys. Lett.* **86** 241111
[8] Tsukazaki A, Kubota M, Ohtomo A, Onuma T, Ohtani K, Ohno H, Chichibu S F and Kawasaki M 2005 *Japan. J. Appl. Phys.* **44** L643
[9] Yang T L, Zhang D H, Ma J, Ma H L and Chen Y 1998 *Thin Solid Films* **326** 60
[10] Ott A W and Chang R P H 1999 *Mater. Chem. and Phys.* **58** 132
[11] Yadav H K, Sreenivas K and Gupta V 2007 *Appl. Phys. Lett.* **90** 172113
[12] Coppa B J, Davis R F and Nemanich R J 2003 *Appl. Phys. Lett.* **82** 400
[13] Kim S H, Kim H K and Seong T Y 2005 *Appl. Phys. Lett.* **86** 022101
[14] von Wenckstern H, Kaidashev E M, Lorenz M, Hochmuth H, Biehne G, Lenzner J, Gottschalch V, Pickenhain R and Grundmann M 2004 *Appl. Phys. Lett.* **84** 79
[15] Oh M S, Hwang D K, Lim J H, Choi Y S and Park S J 2007 *Appl. Phys. Lett.* **91** 042109
[16] Polyakov A Y, Smirnov N B, Kozhukhova E A, Vdovin V I, Ip K, Heo Y W, Norton D P and Pearton S J 2003 *Appl. Phys. Lett.* **83** 1575
[17] von Wenckstern H, Biehne G, Rahman R A, Hochmuth H, Lorenz M and Grundmann M 2006 *Appl. Phys. Lett.* **88** 092102
[18] Allen M W, Durbin S M and Metson J B 2007 *Appl. Phys. Lett.* **91** 053512
[19] Brillson L J, Mosbacker H L, Hetzer M J, Strzhemechny Y, Look D C, Cantwell G, Zhang J and Song J J 2008 *Appl. Surf. Sci.* **254** 8000
[20] Gunji R Y, Nakano M, Tsukazaki A, Ohtomo A, Fukumura T and Kawasaki M 2008 *Appl. Phys. Lett.* **93** 012104
[21] Mridha S and Basak D 2008 *Appl. Phys. Lett.* **92** 142111
[22] Frenzel H, Lajn A, Brandt M, von Wenckstern H, Biehne G, Hochmuth H, Lorenz M and Grundmann M 2008 *Appl. Phys. Lett.* **92** 192108
[23] Li C, Li Y, Wu Y, Ong B S and Loutfy R O 2007 *J. Appl. Phys.* **102** 076101
[24] Ip K, Thaler G T, Yang H, Han S Y, Li Y, Norton D P, Pearton S J, Jang S and Ren F 2006 *J. Cryst. Growth* **287** 149
[25] Özgür Ü, Alivov Y I, Liu C, Teke A, Reshchikov M A, Doğan S, Avrutin V, Cho S J and Morkoç H 2005 *J. Appl. Phys.* **98** 041301
[26] Liu W R, Hsieh W F, Hsu C H, Liang K S and Chien F S S 2006 *J. Cryst. Growth* **297** 294
[27] Sun X W and Kwok H S 1999 *J. Appl. Phys.* **86** 408
[28] Chen J J, Anderson T J, Jang S, Ren F, Li Y J, Kim H S, Gila B P, Norton D P and Pearton S J 2006 *J. Electrochem. Soc.* **153** G462
[29] Brandt M *et al* 2008 *J. Appl. Phys.* **104** 013708
[30] Ip K, Baik Y W H, Norton D P, Pearton S J and Ren F 2004 *Appl. Phys. Lett.* **84** 544
[31] Lin Y J 2005 *Appl. Phys. Lett.* **86** 122109
[32] Kim S Y, Baik J M, Yu H K and Lee J L 2005 *J. Appl. Phys.* **98** 093707
[33] Tuomisto F, Ranki V, Saarinen K and Look D C 2003 *Phys. Rev. Lett.* **91** 205502
[34] Tuomisto F, Saarinen K, Grasza K and Mycielski A 2006 *Phys. Status. Solidi.* b **243** 794
[35] Kohan A F, Ceder G, Morgan D and Van de Walle C G 2000 *Phys. Rev.* B **61** 15019
[36] Patterson C H 2006 *Phys. Rev.* B **74** 144432
[37] Bylander E G 1978 *J. Appl. Phys.* **49** 1188
[38] Morkoç H 1999 *Nitride Semiconductors and Devices* (Berlin: Springer)
[39] Lin Y J, Lin W X, Lee C T and Chang H C 2006 *Japan. J. Appl. Phys.* **45** 2505
[40] Kim H, Ryou J, Dupuis R D, Lee S N, Park Y, Weon J and Seong T Y 2008 *Appl. Phys. Lett.* **93** 192106
[41] Lin Y J and Hsu C H 2004 *J. Electron. Matter* **33** 1036
[42] Yu L S, Liu Q Z, Xing Q J, Qiao D J, Lau S S and Redwing J 1999 *J. Appl. Phys.* **84** 2099
[43] Ishii H, Sugiyama K, Ito E and Seki K 1999 *Adv. Mater.* **11** 605
[44] Agrawal R and Ghosh S 2006 *Appl. Phys. Lett.* **89** 222114
[45] Kampen T U 2006 *Appl. Phys. A: Mater. Sci. Process.* **82** 457